

# The performance characterization of carbon fiber–reinforced plastic for space applications

Journal of Reinforced Plastics and Composites

2023, Vol. 42(15-16) 844–853

© The Author(s) 2022

Article reuse guidelines:

[sagepub.com/journals-permissions](https://sagepub.com/journals-permissions)

DOI: 10.1177/07316844221141367

[journals.sagepub.com/home/jrp](https://journals.sagepub.com/home/jrp)



Baolong Sun<sup>1</sup> , Chuang Xue<sup>1</sup>, Weihui Shang<sup>2</sup>, Mingxin An<sup>1</sup>, Haojiang Zhao<sup>1</sup> and Hansi Zhang<sup>3</sup>

## Abstract

In this paper, the excellent dimensional stability and vacuum outgassing of high-performance carbon fiber–reinforced plastic (CFRP) were discussed. First, the high-performance resin matrix was obtained by modifying cyanate resin, and the modified cyanate ester was used to make prepreg and laminates. Then, the mechanical property retention rate of laminates reached 90.79% under proton and electron irradiation. The average values of total mass loss and collected volatile condensable material of high-performance CFRP were 0.116% and 0.008%, respectively. Finally, the candidate tube and frame were fabricated based on the ply lay-up design. The candidate tube and frame were subjected to a series of experiments of thermal deformation and hygroscopic deformation to verify the dimensional stability. The thermal deformations of the tube and frame reached 0.468  $\mu\text{m}/\text{m}$  and 4.579  $\mu\text{m}/\text{m}$ , respectively, with a temperature variation of 4°C. The measured hygroscopic deformation of the tube reached 8.16  $\mu\text{m}/\text{m}$  in nearly 3 months. The experimental results show that the high-performance CFRP can be used for precision optical structures of space telescopes.

## Keywords

Dimensional stability, thermal deformation, hygroscopic deformation, vacuum outgassing, CFRP

## Highlights

1. Through modification of cyanate ester and optimization of prepreg process, we obtained carbon fiber–reinforced plastic with excellent retention rate of mechanical property and vacuum outgassing, which were significantly better than the existing level. The retention rate reached 90.79% under the proton and electron irradiation. The average value of total mass loss and collected volatile condensable material reached 0.116% and 0.008%, respectively.
2. We developed characterization methods and corresponding testing equipment for dimensional stability of high-performance carbon fiber–reinforced plastic. The result shows that we can manufacture products with dimensional stability of few micrometers, which can be used for precision optical structures of space telescope.

## Introduction

The need for lightweight design continues to increase in various fields. Structures are made from composites instead of metals, especially in the aerospace field. Because of the low coefficient of thermal expansion, high stiffness, and light weight, high-performance carbon fiber–reinforced plastic (CFRP) materials are the most promising

candidates for stable space structures.<sup>1–6</sup> Taking the space telescope structure as an example, optical components and scientific instruments are mounted on a highly stable truss structure. The temperature-related deformation of each component directly affects the relative position between secondary mirror and primary mirror. The change in relative position directly affects the quality of optical images. Therefore, it is absolutely necessary to ensure the dimensional stability of telescope truss structures.<sup>7–10</sup>

For a given design application, CFRP can be tailored for strength, stiffness, coefficient of thermal expansion, and high reliability. CFRP consists of carbon fiber and polymeric matrix resin. Isotropic materials such as polymers expand equally in all directions, but the fibers used to

<sup>1</sup>Changchun Institute of Optics, Fine Mechanics, and Physics, Chinese Academy of Science, Changchun, China

<sup>2</sup>Changchun Long Aerospace Composite Materials Co., Ltd., Changchun, China

<sup>3</sup>Electromechanical Technology Institute, Jilin Agricultural Machinery Research Institute, Changchun, China

## Corresponding author:

Chuang Xue, Changchun Institute of Optics, Fine Mechanics and Physics, Chinese Academy of Science, 577 Yingkou Rd, Erdao District, Changchun 130033, China.

Email: [xuechuang0510@163.com](mailto:xuechuang0510@163.com)

reinforce the polymer resin matrix, that is, carbon fibers in the case of CFRP, are not isotropic. The oriented fibers, which are stiffer than the matrix, produce a higher composite stiffness in the direction of the fiber orientation than in the transverse direction.<sup>11–13</sup> Thus, the thermal deformation in the axial direction of a CFRP tube can be controlled by combining a fiber of appropriate axial stiffness and negative thermal expansion with the matrix resin of given stiffness and positive thermal expansion. With this premise and a well-controlled ply lay-up, a theoretical zero thermal expansion at a given temperature in the direction of interest can be obtained. For example, Strock<sup>14</sup> and Ozaki et al.<sup>15,16</sup> successfully developed high-precision CFRP pipes with an extremely low coefficient of thermal expansion. Because the resin matrix has a certain degree of hygroscopic properties, its composite materials also show hygroscopic characteristics. During the manufacturing and assembly of space structures, operations are routinely conducted in a clean room with an atmosphere maintained at approximately 50% RH humidity. Under these conditions, the structures absorb moisture until equilibrium is reached. The absorbed moisture molecules in polymer composite materials significantly affect the physical and chemical properties of the matrix and the final performance of composite structures, especially in long-term utilization.<sup>17,18</sup>

The resins for space structure composite materials are mainly epoxy resin and cyanate resin. The carbon fiber composite material of the epoxy resin system has the disadvantages of dimensional stability, moisture absorption, and vacuum outgassing. Cyanate resin is a polymer material with excellent performance. Cyanate resin has the advantages of an extremely low moisture absorption rate, excellent dimensional stability and heat resistance, good mechanical and dielectric properties, and excellent processing performance. Based on these advantages, cyanate resin has been used in satellite structural materials and space optical systems. Cyanate resin gradually replaces epoxy resin as the main resin matrix material for spacecraft composite materials.<sup>19</sup>

In the case of our space telescope structure, the secondary mirror is supported at the required 4.96-m vertex separation from the primary mirror by a lightweight truss structure. The configuration of the truss structure consists of frames, support tubes, and joints. For this structure, it is necessary to achieve long-term dimensional stability for the quality of optical images. Thus, the telescope structure must be stable to a few micrometers, which implies an extremely low coefficient of thermal expansion, where the in-operation telescope temperature does not exceed 4°C based on our level of thermal control. The hygroscopic deformation of tubes does not exceed 10  $\mu\text{m}/\text{m}$  during the entire on-orbit operation period (the operating period of telescope on orbit is 15 years).

The telescope truss structure also introduces strict requirements on the space environment resistance and durability of the composite materials. The retention rate of the mechanical property is more than 85% (the operating period of the telescope on orbit is 15 years), the total mass loss (TML) is less than 0.2%, and the collected volatile condensable material (CVCM) is less than 0.02%. These index requirements are much higher than the requirements of carbon fiber composite materials on conventional spacecraft.

In this paper, the research work of high-performance carbon fiber composite materials was mainly performed to evaluate the typical advantages of high mechanical properties, low vacuum outgassing, low thermal expansion, and low hygroscopic deformation. The purpose of this effort was to support the development of an optical structure with extremely high dimensional stability for our space telescope project. Simultaneously, the high-performance carbon fiber composite materials were subjected to proton and electron irradiation experiments in vacuum to characterize the changes in performance of carbon fiber composite materials under the influence of space environmental factors. The necessary bases were also provided to evaluate the service performance of such materials in the space environment.

## Fabrication of CFRP tube and frame

### *Materials of the laminates*

Carbon fiber-reinforced plastic consists of carbon fibers and polymeric matrix resin. Four types of carbon fibers were used in composite materials: T700SC, T800HB, M40JB, and M55JB (Toray Industries Co., Ltd). The research and development of high-performance resin systems and hot-melt prepregs were performed to fulfill the strict requirements of the space telescope structure.

First, 80 parts by weight of cyanate resin was added into the reactor and stirred at a constant temperature (130°C) to the melting state; then, 10 parts by weight of epoxy resin was added in the stirring state. After an even stirring, the temperature was controlled at 60°C, and the stirring speed was maintained at 500 r/min, 0.0003 parts by weight of dibutyltin dilaurate was added, and 5 parts by weight of carboxylated terminated liquid acrylic rubber was fully evenly mixed. Finally, one part by weight of multi-walled carbon nanotubes was added, stirred for approximately 40 min, and ultrasonicated for 2 h so that the carbon nanotubes were uniformly dispersed in the cyanate resin matrix. Then, the mixture was introduced into a three-roll grinder to grind repeatedly 8–10 times to obtain a modified cyanate resin. Finally, the corresponding curing temperature and time of the modified cyanate resin were obtained through thermal analysis. The basic properties of modified cyanate resin with conventional epoxy resin and cyanate resin is shown in Table 1.

**Table 1.** Mechanical properties of matrix resin.

Property	Epoxy resin	Cyanate resin	Modified cyanate resin
Tensile strength (MPa)	75 ± 5	55 ± 5	73
Tensile modulus (GPa)	3.4 ± 0.4	3.2 ± 0.3	3.2
Impact strength (kJ/m <sup>2</sup> )	15 ± 3	7.3 ± 2	16.4
Elongation at break (%)	3.1 ± 0.3	1.2 ± 0.2	2.4
Moisture absorption (%)	1.5 ± 0.3	0.3 ± 0.3	0.25

According to the abovementioned data, compared with conventional epoxy resin, the modified cyanate ester resin has little difference in mechanical properties, but the moisture absorption performance is significantly improved. Compared with conventional cyanate resin, the tensile strength, impact strength, and elongation at break are significantly improved.

First, the modified cyanate resin was preheated to 70–80°C, and the temperature of the glue tank of the coating machine was set to 85°C. Then, the coating machine was used to form a double-layer adhesive film, and the adhesive film was placed on the prepreg belt preparation machine. The unidirectional carbon fiber yarn was dried at 105°C for 2 h, passed through the yarn frame and tension system, and placed in the middle of the double-layer adhesive film. The hot roll temperature was controlled to 85°C, with an immersion speed of 3–5 m/min and immersion pressure of 2–3 MPa, and maintained the temperature constant for 12 h. Finally, the cyanate resin prepreg was obtained by cooling to room temperature at a cooling rate of 2°C/min. The process parameters aforementioned were strictly controlled to make the performance of modified cyanate resin prepreg more consistent and reliable.

Laminates were fabricated by laying up prepreg sheets of unidirectional T700SC, T800HB, M40JB, and M55JB fibers impregnated with modified cyanate resin (the thickness of single-layer prepreg was 0.1 mm). Zero-degree prepreg sheets were laid up, vacuum-bagged, and autoclave-cured. The curing conditions were 2 h at 110°C, followed by 4 h at 130°C. Referring to the national standard GB/T 3855–2005,<sup>20</sup> a small sample at the end of the laminate, which weighted approximately 0.5 g, was taken and placed into the flask. Then, approximately 35 mL of 98% sulfuric acid was injected into the flask. The flask was placed in the fume hood and heated with a heater. The temperature of the heater was set at 260°C for 6 h. Then, 30% hydrogen peroxide was slowly dropped into the mixed solution until the mixed solution was clear and the fiber floated to the solution surface. Then, the mixed solution was repeatedly pumped and filtered with distilled water until the solution was neutral and washed with acetone. Finally, the pumped filter fiber was placed and filtered into an oven at 150°C to dry for 2 h, the weight of the dried fiber was determined, and the fiber density and mass loss rate were combined to obtain the fiber volume

content according to the calculation formula in the national standard. The fiber volume fractions of the laminates were approximately 60%.

The mechanical properties of the laminates were evaluated in both directions of 0° and 90° to the fiber at room temperature. Based on the technique in GB/T3354-2014,<sup>21</sup> the tensile performance parameters were obtained with a DNS100 testing machine (Sinotest Equipment Co., Ltd). The dimensions were 230 mm × 12.5 mm × 2 mm for the unidirectional laminates of the 0-degree specimen. The dimensions were 170 mm × 25 mm × 2 mm for the unidirectional laminates of 90-degree specimen. The mechanical properties of the unidirectional laminates are shown in Table 2.

### Fabrication of CFRP tube

The tubes applied to high-precision space optical structures were required to remain stable in length under specific thermal conditions. Based on our control level of 4°C temperature variation, the thermal deformation of the tubes in the longitudinal direction does not exceed 0.5 μm/m. The ply design was performed according to the abovementioned technical requirements. The theoretical coefficient of thermal expansion (CTE) absolute value of the tube was less than  $0.125 \times 10^{-6}/^{\circ}\text{C}$ . The negative CTE of tubes was more conducive to the dimensional stability of truss structures. Therefore, the design work was performed with a CTE between  $-0.125 \times 10^{-6}/^{\circ}\text{C}$  and  $-0.05 \times 10^{-6}/^{\circ}\text{C}$ . The theoretical CTE was calculated by the analysis software based on the classic laminate theory of composite materials.

The design evolution revolved around M40JB (or M55JB) in the centerline ply for stiffness and T700SC (or T800HB) in the angle ply for the CTE control and stability. The matrix resin used to fabricate the composites was modified cyanate resin. The lamination angles of the first candidate tube (No. 01) were  $[0/+49/0/0/-49/0]_{2s}$ , the ± 49-degree layer consisted of T700SC prepreg, and the 0-degree layer consisted of M40JB prepreg. The lamination angles of the second candidate tube (No. 02) were  $[0/+69/0/0/-69/0]_{5s}$ , the ± 69-degree layer consisted of T800HB prepreg, and the 0-degree layer consisted of M55JB prepreg.

Because of the high requirements for quantitative control of the tubes in this program, hot-melt prepreg was used for laying and forming to stably control the thickness and fiber

**Table 2.** Mechanical properties of unidirectional laminates.

Material type fiber/resin	Modulus/GPa (0°)	Modulus/GPa (90°)	Strength/MPa (0°)	Strength/MPa (90°)
M40JB/modified cyanate	210.2	7.3	1865.3	36.4
M55JB/modified cyanate	305.8	6.7	1320.4	30.6
T700SC/modified cyanate	123.3	9.0	2050.2	45.5
T800HB/modified cyanate	177.5	9.2	2277.8	57.8

volume content. The curing conditions were 110°C for 2 h, followed by curing at 130°C for 4 h. After being cured in an oven, the mandrel was removed. The fiber volume fractions of the tubes were approximately 60%. The length of the No. 01 tube (M40JB/T700SC) was 577 mm, the outer diameter was 80 mm, and the wall thickness was 2.4 mm. The length of the No. 02 tube (M55JB/T800HB) was 2008 mm, the outer diameter was 80 mm, and the wall thickness was 5 mm. Figure 1 shows a photograph of the tubes.

### Fabrication of the CFRP frame

The frame applied to high-precision space optical structures was required to remain stable in length under specific thermal conditions. The carbon fiber applied to the frame was high-modulus M40JB fiber. The matrix resin to fabricate the composites was modified cyanate resin. The layup method adopted a quasi-isotropic layup design. The curing conditions were 2 h at 110°C, followed by 4 h at 130°C. After curing in an oven, the mold was removed. The fiber volume fractions of the frame were approximately 60%. The frame (M40JB) was 802 mm long, 140 mm wide, 80 mm high, and the wall thickness was 6 mm. Figure 2 shows a photograph of the frame.

## Experiment

### Retention rate of mechanical property

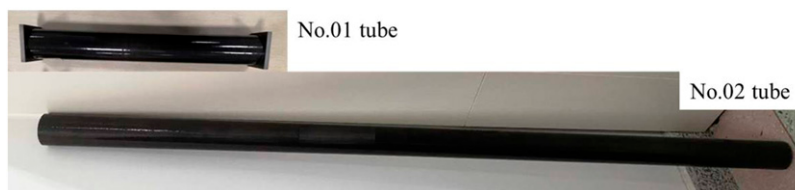
For our telescope project, there was a protective skin outside of the precision optical structure. Therefore, the precision optical structure was mainly exposed to vacuum proton and electron irradiation in the space environment. To evaluate the performance evolution of composite materials in a space environment, a space integrated radiation simulator was used to obtain the proton and electron irradiation

environment for specimens. After the proton and electron irradiation experiment, the technical index requirement of the retention rate of mechanical property was more than 85%.

The ply lay-up design was consistent with the aforementioned tubes and frame. The lamination angles of the first type specimen were  $[0/+69/0/-69/0]_{2s}$ , the  $\pm 69$ -degree layer was consisted of T800HB prepreg, and the 0-degree layer consisted of M55JB prepreg. The 0-degree layer was along the length of the specimen. The lamination angles of the second type specimen were  $[0/+60/-60]_2 [0/90/+45/-45]_s [-60/+60/0]_2$ , each layer consisted of M40JB prepreg, and the 0-degree layer was along the length of the specimen. The curing conditions were 2 h at 110°C, followed by 4 h at 130°C. The fiber volume fractions of the specimen were approximately 60%. The dimensions of the tensile specimen were 230 mm  $\times$  25 mm  $\times$  2 mm. The tensile modulus of the specimen before and after the proton and electron irradiation experiments was evaluated with a DNS100 testing machine (Sinotest Equipment Co., Ltd) at room temperature. The total dose of space proton irradiation was  $3.36 \times 10^7$  rad (Si). The proton irradiation intensity was  $1.68 \times 10^7$  rad (Si)/h. The proton irradiation period was maintained at 2 h. The total dose of space electron irradiation was  $3.26 \times 10^7$  rad (Si). The electron irradiation intensity was  $3.1 \times 10^5$  rad (Si)/h. The electron irradiation period was maintained at 105 h.

### Total mass loss and collected volatile condensable material

In the vacuum environment of space, unreacted additives, impurities, gas, or water vapor adsorbed on the surface and inside of the material would cause material outgassing. The problem of outgassing pollution directly affected the normal and stable operation of precision optical systems. In the case

**Figure 1.** Photograph of the CFRP tube.



**Figure 2.** Photograph of the CFRP frame.

of our telescope structure, the technical index requirement of total mass loss (TML) is less than 0.2%, and the technical index requirement of collected volatile condensable material (CVCM) is less than 0.02%.

The lamination angles of the specimen were  $[0]_{20}$ , and each layer consisted of M55JB prepreg. The curing conditions were 2 h at 110°C, followed by 4 h at 130°C. The fiber volume fractions of the specimen were approximately 60%. The specimen was cut into 2 mm × 2 mm × 2 mm cubes. The 800 mg cubes were weighed and divided into four equal parts for testing. According to the technique in ASTM E595-2015,<sup>22</sup> the vacuum outgassing performance of composite materials was tested with pollution condensation effect equipment and electronic microbalance. The specimens for evaluating the volatile content of the material were subjected to 125°C at  $1 \times 10^{-3}$  Pa pressure for 24 h. The accuracy of temperature control was  $\pm 1^\circ\text{C}$ . The overall mass loss was classified into noncondensable and condensable. The latter was characterized herein as being capable of condensing on a collector at a temperature of 25°C. The accuracy of temperature control was  $\pm 1^\circ\text{C}$ .

### Thermal deformation

To achieve long-term dimensional stability for observation, the telescope structure must be stable to a few micrometers. The configuration of the truss structure consists of frames, support tubes, and joints. Based on our control level of 4°C temperature variation, the thermal deformation of the tubes in the longitudinal direction does not exceed 0.5  $\mu\text{m}/\text{m}$ , and the thermal deformation of the frames in the longitudinal direction does not exceed 5  $\mu\text{m}/\text{m}$ .

A high-precision measurement apparatus based on laser interferometry was developed. The apparatus measured dimensional changes with nanometer sensitivity to characterize the thermal deformation of highly stable materials. The apparatus used a displacement measuring interferometer (DMI) system to measure the length variation and a PT100 temperature sensor to record the temperature variation. The specimen was maintained inside a vacuum vessel with a temperature control unit to simulate the space thermal environment. An optical window was installed on the vacuum vessel for the laser light to pass through. The entire apparatus was placed in a clean room with constant

temperature and humidity. The error of the temperature measuring system was approximately 0.102°C. The deviation of the temperature regulation system was approximately 0.3°C. Figure 3 shows a photograph of our apparatus. Our apparatus had excellent repeatability and the correct absolute value. The measurement uncertainty was the  $1.3 \times 10^{-8} \text{ m}/\text{m} \times ^\circ\text{C}$ .<sup>23</sup>

The tubes and frame were subjected to preconditioning prior to testing for stabilization. First, the specimens were dried in a hot vacuum vessel to reduce their moisture content to nearly zero. The specific conditions for the specimens were a temperature of 80°C and a pressure of  $1 \times 10^{-4}$  Pa for several days. Then, 16 thermal cycles were conducted to improve the dimensional stability. The heating and cooling rate of the thermal cycle was 4°C/min. The temperature range of the thermal cycle was from  $-20^\circ\text{C}$  to 60°C. The temperature was maintained for at least 60 min at  $-20^\circ\text{C}$  and 60°C. The temperature was maintained for at least 30 min at 0°C, 20°C, and 40°C. Figure 4 shows the heating and cooling curve of the thermal cycle.

Since our apparatus could simultaneously measure three specimens simultaneously, the No. 01 tube (M40JB/T700SC), No. 02 tube (M55JB/T800HB), and frame (M40JB) were placed inside a vacuum vessel with temperature control. The specimens for evaluating the thermal deformation were subjected to a  $1 \times 10^{-2}$  Pa pressure with 4°C temperature variation.

### Hygroscopic deformation

For this project, the modified cyanate resin system was used as the resin matrix, which has hygroscopic properties. The composite materials also show hygroscopic characteristics, which will affect the long-term dimensional stability. The technical index requirement of hygroscopic deformation is less than 10  $\mu\text{m}/\text{m}$ .

A high-accuracy measurement device was developed to characterize the hygroscopic deformation of highly stable materials induced by moisture absorption. The measurement device measured dimensional changes induced by moisture absorption with submicron sensitivity based on a high-resolution grating ruler. Figure 5 shows a schematic of the present hygroscopic deformation measurement system. The measurement device used a high-resolution grating ruler to measure the length variation at room temperature and a temperature and humidity recording instrument to record ambient temperature and humidity variation. The resolution of the grating ruler was 0.1  $\mu\text{m}$ , and the measuring uncertainty was  $\pm 0.3 \mu\text{m}$ .

The displacement measuring system of our device was composed of a grating ruler, the grating ruler support, specimen support, mounting base, and supporting electronics. The grating ruler converted the linear displacement changes into a pulse signal. The number of pulse signals corresponded to the displacement of movement. The entire



**Figure 3.** High-precision measurement apparatus.

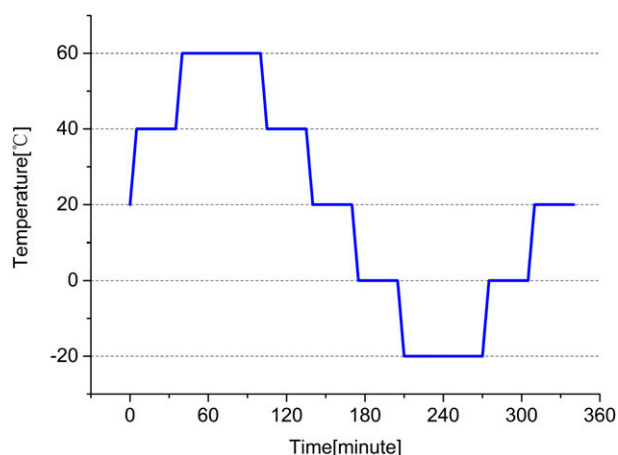


**Figure 4.** Heating and cooling curve of the thermal cycle.

apparatus was placed in a constant temperature and humidity chamber. Figure 6 shows a photograph of the hygroscopic deformation measurement device.

The No. 01 tube was placed inside the hygroscopic deformation measurement device with temperature and humidity control. The measurement device maintained a relative humidity of 55% RH at room temperature to simulate the manufacturing and assembly environment of the CFRP structures.

## Results and discussion

### Results of the retention rate of mechanical properties

The tensile modulus of the specimen before and after the proton and electron irradiation experiments was evaluated

with a DNS100 testing machine (Sinotest Equipment Co., Ltd). Table 3 shows the retention rates of the mechanical properties of the specimens.

The average retention rate for mechanical properties was 90.79%, which was higher than the technical index requirement of 85%. The experimental results show that our high-performance carbon fiber-reinforced plastic has excellent mechanical properties under proton and electron irradiation environments.

### Result of the total mass loss and collected volatile condensable material

The test of vacuum outgassing performance of composite materials was performed with pollution condensation effect equipment and an electronic microbalance. Table 4 shows the results of the total mass loss and collected volatile condensable material of the specimen.

The average TML was 0.116%, which was far lower than the technical index requirement of 0.2%. The average CVCVM was 0.008%, which was far lower than the technical index requirement of 0.02%. The experimental results show that our high-performance carbon fiber-reinforced plastic has excellent properties of vacuum outgassing.

### Results of the thermal deformation test

To characterize the thermal deformation of the aforementioned tubes and frame, the tubes and frame were placed inside a vacuum vessel with temperature control. The temperature variation was close to 4°C. Figure 7 shows the experimental curves of tubes No. 01 and No. 02. Figure 8 shows the experimental curve of the frame.

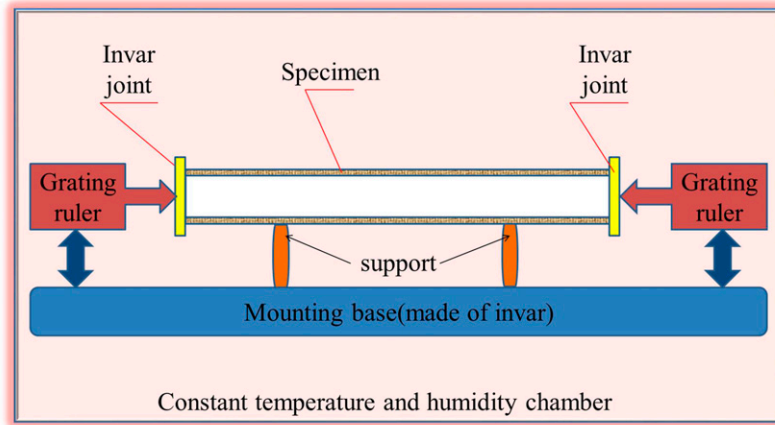


**Figure 5.** Schematic representation of the hygroscopic deformation measurement.

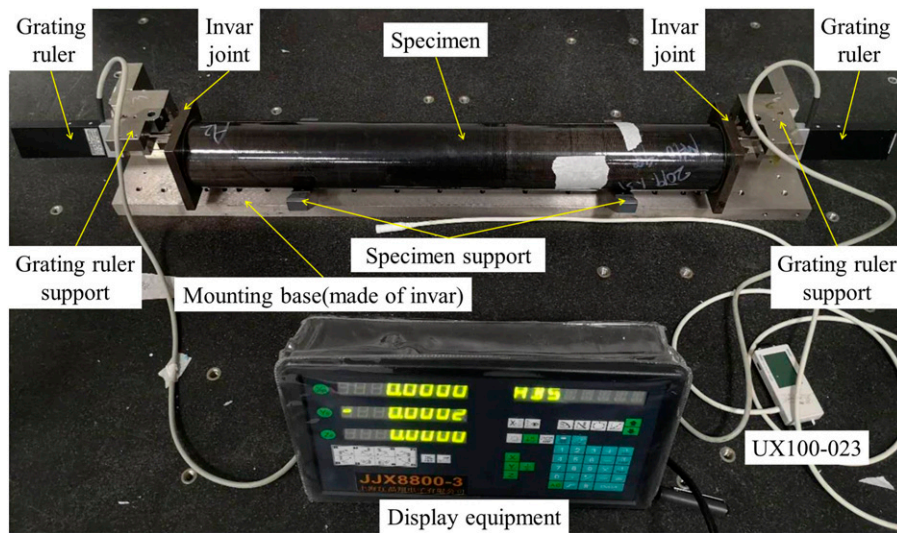


**Figure 6.** Hygroscopic deformation measurement device.

**Table 3.** Result of the retention rate of mechanical property.

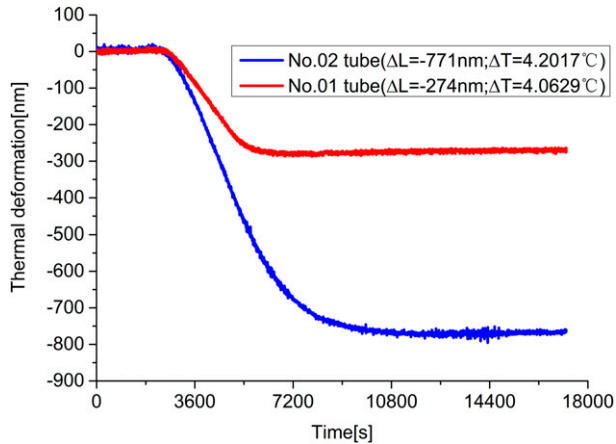
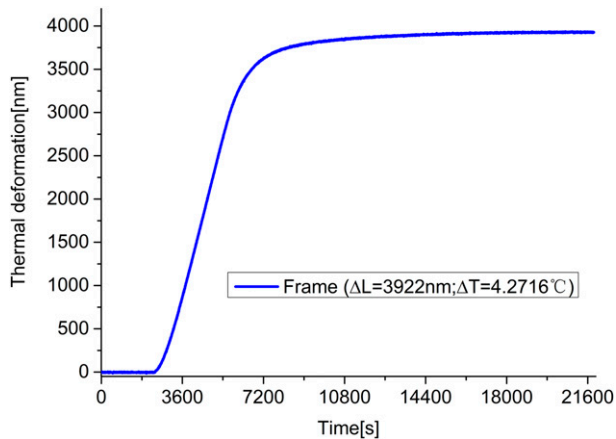
Serial number of specimen under tensile modulus test	Modulus/GPa (before the proton and electron irradiation)	Modulus/GPa (after the proton and electron irradiation)	Percentage/% (modulus retention rate)
First type—No. 01	182.93	165.37	90.40
First type—No. 02	179.68	159.88	88.98
First type—No. 03	180.79	171.31	94.76
Second type—No. 01	85.93	80.92	94.17
Second type—No. 02	89.30	78.51	87.92
Second type—No. 03	96.28	85.22	88.51
Average			90.79

The measured thermal deformation  $\Delta L$  of tube No. 01 was  $-274$  nm ( $L_0 = 577$  mm,  $\Delta T = 4.0629^\circ\text{C}$ ). The measured thermal deformation  $\Delta L$  of tube No. 02 was  $-771$  nm ( $L_0 = 2008$  mm,  $\Delta T = 4.2017^\circ\text{C}$ ). The measured thermal

deformation  $\Delta L$  of the frame was  $3922$  nm ( $L_0 = 802$  mm,  $\Delta T = 4.2716^\circ\text{C}$ ). The measurement results were normalized to obtain the thermal deformation at a standard length of  $1$  m and a temperature variation of  $4^\circ\text{C}$ . As shown in Table 5, the

**Table 4.** Result of the total mass loss and collected volatile condensable material.

Serial number of specimen	TML/%	CVCM/%
Specimen—No. 01	0.121	0.005
Specimen—No. 02	0.112	0.004
Specimen—No. 03	0.118	0.015
Specimen—No. 04	0.113	0.008
Average	0.116	0.008

**Figure 7.** Thermal deformation curves of the tubes No. 01 and No. 02.**Figure 8.** Thermal deformation curves of the frame.**Table 5.** Normalized result of the thermal deformation.

Serial number of specimen	Normalization of test results ( $\mu\text{m}/\text{m}$ )	Technical index requirement ( $\mu\text{m}/\text{m}$ )
Tube No. 01	0.468	0.5
Tube No. 02	0.366	0.5
Frame	4.579	5

normalized results were  $0.468 \mu\text{m}/\text{m}$  (No. 01 tube),  $0.366 \mu\text{m}/\text{m}$  (No. 02 tube), and  $4.579 \mu\text{m}/\text{m}$  (frame).

The normalized measurements of thermal deformation for tubes were  $0.468 \mu\text{m}/\text{m}$  and  $0.366 \mu\text{m}/\text{m}$ , which were lower than the technical index requirement of  $0.5 \mu\text{m}/\text{m}$ . The normalized measurement of thermal deformation for the frame was  $4.579 \mu\text{m}/\text{m}$ , which was lower than the technical index requirement of  $5 \mu\text{m}/\text{m}$ . The measured results show that our high-performance carbon fiber-reinforced plastic has excellent dimensional stability under specific thermal conditions. According to the result of software ply design, the greater of ply angle design or the smaller of ply angle design will all lead to an increase in thermal deformation.

### Result of hygroscopic deformation test

The test of hygroscopic deformation of tube No. 01 was performed with a self-developed high-accuracy measurement device subjected to a relative humidity of 55% RH at room temperature. A temperature and humidity recording instrument was used to record the changes in ambient temperature and relative humidity during the hygroscopic experiment. Figure 9 shows the recording result of ambient temperature and relative humidity. Figure 10 shows the hygroscopic deformation of tube No. 01 over nearly 3 months.

The recorded fluctuation of temperature was close to  $0.3^\circ\text{C}$ , which was far lower than the technical index requirement of  $\pm 3^\circ\text{C}$  in ASTM D5529/D5529M-2014.<sup>24</sup> The deformation error induced by the temperature fluctuation of tube No. 01 was approximately  $0.02 \mu\text{m}$ , which was far lower than the grating ruler resolution of  $0.1 \mu\text{m}$ . Therefore, the deformation error induced by temperature fluctuation can be negligible.

The measured hygroscopic deformation  $\Delta L$  of tube No. 01 was  $4.7 \mu\text{m}$  ( $L_0 = 577 \text{ mm}$ ) over nearly 3 months. The measurement result was normalized to obtain the hygroscopic deformation at a standard length of 1 m. The normalized measurement of hygroscopic deformation for tube No. 01 was  $8.16 \mu\text{m}/\text{m}$ , which was lower than the technical index requirement of  $10 \mu\text{m}/\text{m}$ . According to the result of software ply design, the greater of ply angle design will lead to an increase in hygroscopic deformation and the smaller of ply angle design will lead to a decrease in hygroscopic deformation.



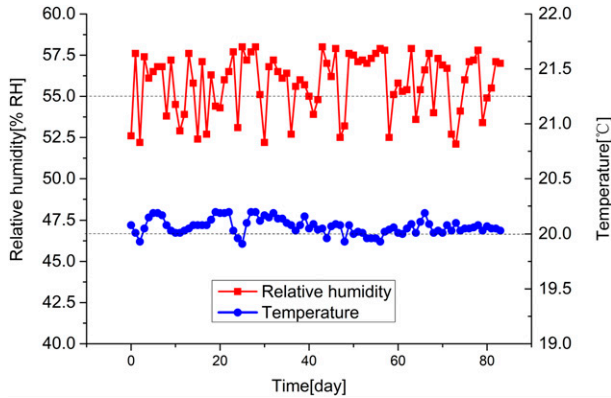


**Figure 9.** Temperature and relative humidity record of UX100-023.

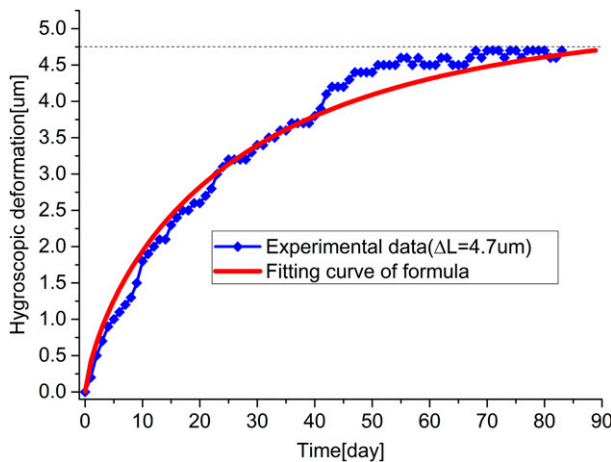


**Figure 10.** Time-dependent hygroscopic deformation.

The hygroscopic deformation curve grows very slowly, which is very close to the equilibrium of hygroscopic deformation. According to the analytic model of Shen and Springer,<sup>25–27</sup> the relationship between hygroscopic deformation  $\Delta L$  and maximum hygroscopic deformation  $L_{\max}$  can be related by the following formula:

$$\Delta L = L_{\max} * \left\{ 1 - \exp \left[ -7.3 * \left( \frac{D_x * t}{S^2} \right)^{0.75} \right] \right\} \quad (1)$$

where  $\Delta L$  is the hygroscopic deformation of tube No. 01 at any time  $t$ ,  $L_{\max}$  is the maximum hygroscopic deformation,  $S$  is the section thickness of tube No. 01, and  $D_x$  is the hygroscopic diffusivity.

Based on the aforementioned formula and experimental data, multi-parameter fitting was conducted to obtain the maximum hygroscopic deformation  $L_{\max}$ . The fitting result shows that  $L_{\max}$  was 5.16  $\mu\text{m}$ , and the measured hygroscopic deformation 4.7  $\mu\text{m}$  reached more than 91% of the maximum hygroscopic deformation 5.16  $\mu\text{m}$ . The fitting

result was normalized to obtain the maximum hygroscopic deformation at a standard length of 1 m. The normalized fitting result was 8.94  $\mu\text{m}/\text{m}$ . Therefore, the maximum hygroscopic deformation of the No. 01 tube was lower than 9  $\mu\text{m}/\text{m}$ . The experimental and analysis results show that our high-performance carbon fiber-reinforced plastic has excellent long-term dimensional stability.

## Conclusion

The mechanical property retention rate of high-performance carbon fiber-reinforced plastic reached 90.79% under proton and electron irradiation, which was higher than the indicator 85% of conventional composite materials. The average total mass loss and average collected volatile condensable material of high-performance carbon fiber-reinforced plastic were 0.116% and 0.008%, respectively, which were far lower than the conventional composite materials. The thermal deformation of the tube reached 0.468  $\mu\text{m}/\text{m}$  with a temperature variation of 4°C. The thermal deformation of the frame reached 4.579  $\mu\text{m}/\text{m}$  with a temperature variation of 4°C. The measured hygroscopic deformation of the tube reached 8.16  $\mu\text{m}/\text{m}$  in nearly 3 months, and the maximum hygroscopic deformation was lower than 9  $\mu\text{m}/\text{m}$  based on the multi-parameter fitting of the experimental data. The excellent thermal and hygroscopic stabilities were verified.

The experimental results show that this material and structure have sufficient performance to support the development of an optical structure with extremely high dimensional stability for our space telescope project. Based on the results, the necessary basis for the service performance evaluation of such materials in the space environment was also provided. The design and fabrication of an optical structure based on this high-performance carbon fiber-reinforced plastic of our space telescope are in progress.

## Declaration of conflicting interests

The author(s) declared no potential conflicts of interest with respect to the research, authorship, and/or publication of this article.

## Funding

The author(s) disclosed receipt of the following financial support for the research, authorship, and/or publication of this article: This work is supported by the program “Research on Preparation Technology of High Performance Carbon Fiber Composite Material” of Changchun Institute of Optics, Fine Mechanics and Physics, Chinese Academy of Science.

## ORCID iD

Baolong Sun  <https://orcid.org/0000-0003-1261-191X>

## References

1. Qian Y, Hao X, Shi Y, et al. Deformation behavior of high accuracy carbon fiber-reinforced plastics sandwiched panels at low temperature. *J Astron Telesc Instr Syst* 2019; 5(3): 034003. DOI: [10.1117/1.JATIS.5.3.034003](https://doi.org/10.1117/1.JATIS.5.3.034003)
2. Hong H, Bae KJ, Jung H, et al. Preparation and characterization of carbon fiber reinforced plastics (CFRPs) incorporating through-plane-stitched carbon fibers. *Compos Struct* 2022; 284: 115198. DOI: [10.1016/j.compstruct.2022.115198](https://doi.org/10.1016/j.compstruct.2022.115198)
3. Nawab Y, Jacquemin F, Casari P, et al. Study of variation of thermal expansion coefficients in carbon/epoxy laminated composite plates. *Compos B Eng* 2013; 50: 144–149. DOI: [10.1016/j.compositesb.2013.02.002](https://doi.org/10.1016/j.compositesb.2013.02.002)
4. Jung H, Choi HK, Lee HS, et al. High strain rate effects on mechanical properties of inductively coupled plasma treated carbon nanotube reinforced epoxy composites. *Compos B Eng* 2018; 154: 209–215. DOI: [10.1016/j.compositesb.2018.08.015](https://doi.org/10.1016/j.compositesb.2018.08.015)
5. Wang R, Wu Q, Xiong K, et al. Evaluation of the matrix crack number in carbon fiber reinforced plastics using linear and nonlinear acousto-ultrasonic detections. *Compos Struct* 2021; 255: 112962. DOI: [10.1016/j.compstruct.2020.112962](https://doi.org/10.1016/j.compstruct.2020.112962)
6. Xiang YX, Shen K, Wu H, et al. Preparation of fixed length carbon fiber reinforced plastic composite sheets with isotropic mechanical properties. *New Carbon Mater* 2021; 36(6): 1188–1194. DOI: [10.1016/S1872-5805\(21\)60094-X](https://doi.org/10.1016/S1872-5805(21)60094-X)
7. Lallo MD. Experience with the hubble space telescope: 20 years of an archetype. *Opt Eng* 2012; 51(1): 011011. DOI: [10.1117/1.OE.51.1.011011](https://doi.org/10.1117/1.OE.51.1.011011)
8. Kitamoto K, Kamiya T and Mizutani T. Evaluation of dimensional stability of metering truss structure using built-in laser interferometric dilatometer. *Eng Res Express* 2020; 2(4): 045023. DOI: [10.1088/2631-8695/abc9cf](https://doi.org/10.1088/2631-8695/abc9cf)
9. Moisheev AA and Shostak SV. On the development of transformable structures of space telescopes. *Solar Syst Res* 2020; 54(7): 707–711. DOI: [10.1134/S0038094620070151](https://doi.org/10.1134/S0038094620070151)
10. An M, Zhang L, Xu S, et al. Design, analysis, and testing of kinematic mount for astronomical observation instrument used in space camera. *Rev Sci Instr* 2016; 87(11): 114501. DOI: [10.1063/1.4966674](https://doi.org/10.1063/1.4966674)
11. Kim RY, Crasto AS and Schoeppner GA. Dimensional stability of composite in a space thermal environment. *Compos Sci Technol* 2000; 60(12–13): 2601–2608. DOI: [10.1016/S0266-3538\(00\)00052-X](https://doi.org/10.1016/S0266-3538(00)00052-X)
12. Sanjuan J, Preston A, Korytov D, et al. Carbon fiber reinforced polymer dimensional stability investigations for use on the laser interferometer space antenna mission telescope. *Rev Sci Instr* 2011; 82(12): 124501. DOI: [10.1063/1.3662470](https://doi.org/10.1063/1.3662470)
13. Ozaki T, Ikeda C, Isoda M, et al. New high-thermal-conductivity composite material for high-precision space optics: missions to the sun, *SPIE*, 2804, 1996, 22–31. DOI: [10.1117/12.259709](https://doi.org/10.1117/12.259709)
14. Strock JD. Development of zero coefficient of thermal expansion composite tubes for stable space structures. *Des Opt Instr SPIE* 1992; 1690: 223–230. DOI: [10.1117/12.137997](https://doi.org/10.1117/12.137997)
15. Ozaki T, Naito K, Mikami I, et al. High precision composite pipes for SOLAR-B optical structures. *Acta Astronaut* 2001; 48(5–12): 321–329. DOI: [10.1016/S0094-5765\(01\)00027-3](https://doi.org/10.1016/S0094-5765(01)00027-3)
16. Ozaki T and Hahn S. Composite materials for extremely large mirrors and optical structures second backaskog workshop on extremely large telescopes. *SPIE* 2004; 5382: 305–312. DOI: [10.1117/12.566319](https://doi.org/10.1117/12.566319)
17. Kim JK, Hu C, Woo RS, et al. Moisture barrier characteristics of organoclay–epoxy nanocomposites. *Compos Sci Technol* 2005; 65(5): 805–813. DOI: [10.1016/j.compscitech.2004.10.014](https://doi.org/10.1016/j.compscitech.2004.10.014)
18. Mára V, Michalcová L, Kadlec M, et al. The effect of long-time moisture exposure and low temperatures on mechanical behavior of open-hole Cfrp laminate. *Polym Compos* 2021; 42(7): 3603–3618. DOI: [10.1002/pc.26082](https://doi.org/10.1002/pc.26082)
19. Arao Y, Fukui T, Niwa T, et al. Dimensional stability of epoxy-based and cyanate-based carbon fiber-reinforced plastics. *J Compos Mater* 2015; 49(12): 1483–1492. DOI: [10.1177/0021998314535455](https://doi.org/10.1177/0021998314535455)
20. GB/T 3855-2005. Test method for resin content of fiber reinforced plastics, 2005.
21. GB/T 3354-2014. Test method for tensile properties of orientation fiber reinforced polymer matrix composite materials, 2014.
22. ASTM E595-2015. Standard test method for total mass loss and collected volatile condensable materials from outgassing in a vacuum environment, 2015.
23. Sun B, Zhang H, Xue C, et al. A high-precision apparatus for dimensional characterization of highly stable materials in space applications. *Mech Adv Mater Struct* 2021; 29: 1–14. DOI: [10.1080/15376494.2021.1926605](https://doi.org/10.1080/15376494.2021.1926605)
24. ASTM D5529/D5529M-2014. Standard test method for moisture absorption properties and equilibrium conditioning of polymer matrix composite materials, 2014.
25. Shen CH and Springer GS. Moisture absorption and desorption of composite materials. *J Compos Mater* 1976; 10(1): 2–20.
26. Shen CH and Springer GS. Environmental effects on the elastic moduli of composite materials. *J Compos Mater* 1977; 11(3): 250–264.
27. Facey T, Defilippis N and Young P. Moisture loss from graphite structures for the Hubble Space Telescope. In Proceedings of the Shuttle Environment and Operations II Conference, November, 1985, Houston, TX, pp. 13–17. DOI: [10.2514/6.1985-6057](https://doi.org/10.2514/6.1985-6057)